AJNR

Definition of the Ostium (Neck) of an Aneurysm Revealed by Intravascular Sonography: An Experimental Study in Canines

Aquilla S. Turk, Charles M. Strother, Daniel I. Crouthamel and James A. Zagzebski

AJNR Am J Neuroradiol 1999, 20 (7) 1301-1308
http://www.ajnr.org/content/20/7/1301

AJNR Am J Neuroradiol 20:1301–1308, August 1999

Definition of the Ostium (Neck) of an Aneurysm Revealed by Intravascular Sonography: An Experimental Study in Canines

Aquilla S. Turk, Charles M. Strother, Daniel I. Crouthamel, and James A. Zagzebski

BACKGROUND AND PURPOSE: **The major factor influencing the effectiveness of Guglielmi detachable coils (GDCs) in the treatment of saccular aneurysms is the size of the aneurysm's ostium (neck). Current imaging techniques often do not allow accurate assessment of aneurysm neck morphology. The primary purpose of this study was to determine the feasibility of using intravascular sonography to provide this information.**

METHODS: **Lateral and bifurcation aneurysms were created in each of six adult mongrel dogs by using a well-established surgical technique. Aneurysms were evaluated with digital subtraction angiography and intravascular sonography before (n = 12) and after (n = 6) treatment with GDCs. Angiography was performed using standard techniques. Sonography was performed using both a commercially available 2.6F 40-MHz catheter and a preproduction 0.014-inch 40-MHz imaging core wire housed in a Tracker catheter. Angiograms and sonograms were reviewed independently by two observers to assess the clarity and accuracy with which they depicted the size of each aneurysm's ostium. Posttreatment intravascular sonograms were evaluated for the extent to which they depicted the completeness of aneurysm obliteration. Two-dimensional reformatted images were made of the intravascular sonographic pullback sequences.**

RESULTS: **In all instances, intravascular sonography provided clear definition of the aneurysm's neck (ostium) morphology as well as its relationship to the parent artery and adjacent branches, especially when 2D reformatted images were obtained. The position of coils in aneurysms was also clearly defined.**

CONCLUSION: **Intravascular sonography is a novel technique for viewing the ostium (neck) of an aneurysm. It provides information not available with current angiographic methods.**

Over the last decade, largely because of the availability of Guglielmi detachable coils (GDCs), endovascular treatment has become a key component in the armamentarium used to treat saccular intracranial aneurysms (1–3). Successful and effective endovascular treatment of saccular aneurysms with GDCs requires knowledge of the aneurysm's neck size and of the relationship between the origin of the aneurysm, its parent artery, and adjacent branches (4). When aneurysms are large, have a complex shape, or are located at a bifurcation where vascular branching is complex, it is often difficult or even impossible to define these morphologic features by using currently available imaging technology. Intravascular sonography has become an important tool both for analysis of vascular lesion characteristics and guidance of therapeutic interventions in the coronary arteries and peripheral vascular system. The primary purpose of our study was to evaluate the feasibility of using intravascular sonography to measure the size of the aneurysm's ostium and to establish its relationship to the parent artery and adjacent arterial branches.

Received September 30, 1998; accepted after revision March 9, 1999.

Technical and financial support provided by Target Therapeutics/Boston Scientific, Inc, Natick MA, of which Dr. Strother is a member of the Scientific Advisory Board.

Recipient of the Dyke Award at the annual meeting of the American Society of Neuroradiology, San Diego, May 1999.

From the Department of Radiology, University of Wisconsin Health Sciences Center, E1/320, 600 Highland Ave, Madison, WI 53792.

Address reprint requests to Charles M. Strother, MD.

Methods

Aneurysm Creation

Under an institutionally approved animal protocol, one lateral and one bifurcation aneurysm were created in each of six

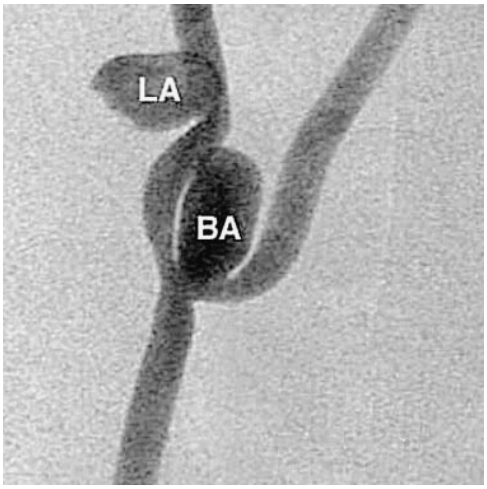

FIG 1. Digital subtraction angiogram of lateral (*LA*) and bifurcation (*BA*) aneurysms in a canine model. This image was obtained with a portable C-arm device.

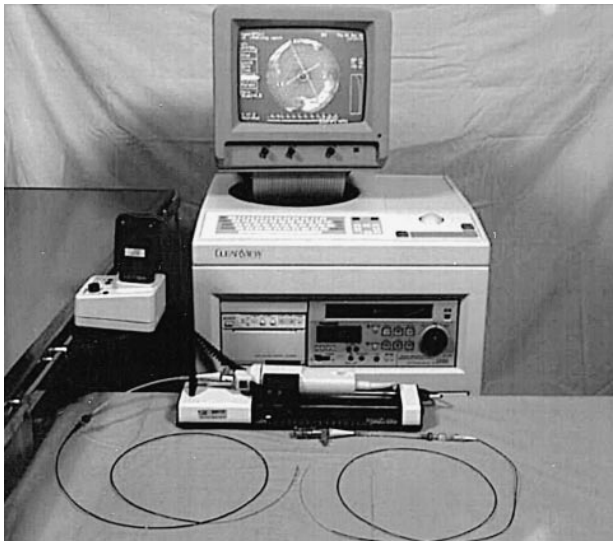

FIG 2. Intravascular sonographic machine with automated pullback servo and catheters.

adult female mongrel dogs (Fig 1). The technique used was that first reported by German and Black (5); it has been developed further in our laboratory over the last 9 years (6). For construction of the ostium of each of the lateral aneurysms, the arteriotomy onto which the vein patch was attached was made by using an arterial punch with a diameter of 5 mm. For construction of the ostium of the bifurcation aneurysms, an attempt was made to standardize the arteriotomy onto which the vein patch was to be attached so that its greatest diameter measured between 6 and 8 mm.

Intravascular Sonography and Angiographic Imaging

In all instances, an interval of at least 3 weeks elapsed between creation of the aneurysms and examination with intravascular sonography. With animals under endotracheal halothane anesthesia, vascular access was obtained through insertion of a 6F or 7F sheath into both common femoral arteries. Fluoroscopy and digital subtraction angiography (DSA) were performed using either a portable C-arm or a biplane fluoroscopic system. Angiograms were obtained in at least two projections, with efforts made to optimize visualization of the relationship of each aneurysm to its parent artery. In two instances, rotational angiography was also performed. Intravascular sonography was performed with the Clear View Ultra system (SciMed/Boston Scientific Corp, Boston, MA) with either a 2.6F 40-MHz catheter (Discovery, Boston Scientific Corp) or a preproduction 0.014-inch 40-MHz imaging core wire (Boston Scientific) housed in a Tracker catheter (Target Therapeutics/Boston Scientific Corp) (Fig 2). To allow introduction of the ultrasound transducer into the dome of the bifurcation aneurysm, it was necessary to trim the distal end of the Discovery catheter to the point where the transducer just remained housed inside the catheter. The imaging core wire was matched in length to that of the Tracker catheter so that the transducer was located just proximal to the catheter's distal tip marker. Both intravascular sonographic catheters consist of a mechanical motor-driven rotating transducer (1800 rpm) that is mounted on a flexible drive shaft. The Discovery catheter is compatible with a 0.014-inch guidewire.

For all intravascular sonographic examinations, a 6F guiding catheter was positioned in the right common carotid artery with its tip at a location several centimeters below the site of the aneurysms. Following creation of an angiographic roadmap, the intravascular sonographic catheter was introduced through the guiding catheter and advanced so that it was either inside the dome of a bifurcation aneurysm or in the parent artery alongside a lateral aneurysm. To facilitate orientation of the ultrasound transducer in a plane perpendicular to an aneurysm's neck (ostium), gentle curves were sometimes formed on both the Discovery and the Tracker catheters. Using a commercially available motorized servo device that pulled back the catheter at a controlled and constant rate (either 1.0 or 0.5 mm/s), intravascular sonograms were obtained as the transducer was moved either out of or alongside each aneurysm. The speed of movement during image acquisition was either 0.5 or 1.0 mm/s. Images were acquired at the rate of 30 frames per second.

In three animals, intravascular sonographic examinations were also done after treatment of the aneurysms with standard GDCs. Coils were placed into the aneurysms by means of standard techniques, and posttreatment intravascular sonograms were obtained in a manner identical to that described above except that no effort was made to introduce the intravascular sonographic catheter into the dome of any of the aneurysms. In one of the lateral and one of the bifurcation aneurysms, coils were purposely positioned so that parent artery compromise was evident on angiographic images.

Data Analysis

Angiograms and sonograms were recorded either on half-inch super VHS videotape, thermal paper, or film. Images were archived either on CDs or floppy disks for off-line reconstruction and analysis. All image analysis was performed off-line, and measurements were made using commercial software with electronic calipers. For intravascular sonographic assessment, each author made measurements independently on two separate occasions. To ensure that measurements were made from the same image by each investigator, a time-dubbed videotape was used. Each observer's determination of ostia dimensions was independently compared using simple regression statistics with StatView (Abacus Concepts, Berkeley, CA). A regression plot was generated both for intraobserver data sets and for interobserver correlation. Because the accuracy of the calibration of the imaging core wire was not known, only images obtained with the Discovery catheter were used for quantitative analysis.

For lateral aneurysms, direct measurements were made of the width of the aneurysm's ostium as well as of the diameter of the parent artery at locations above and below the aneurysm using electronic calipers (Fig 3). The length of each lateral aneurysm ostium was determined from the video recording by

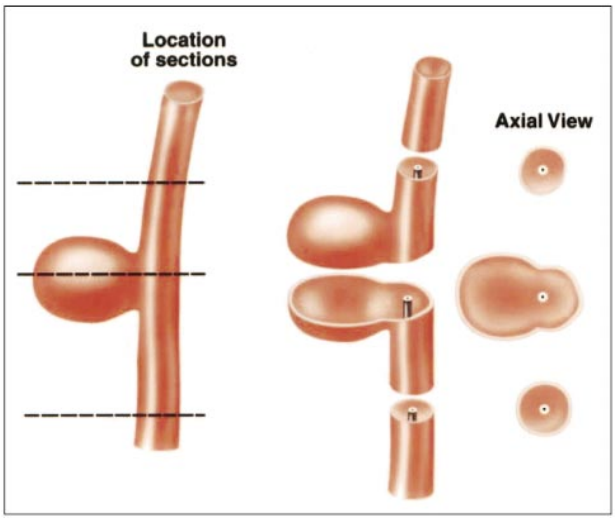

FIG 3. *Left,* Diagram of a lateral aneurysm and parent artery (*dashed lines* indicate locations in which intravascular sonographic measurements were made).

Center, Line drawing of sections through the parent artery and the aneurysm in the plane of intravascular sonography.

Right, Line drawing of corresponding intravascular sonograms.

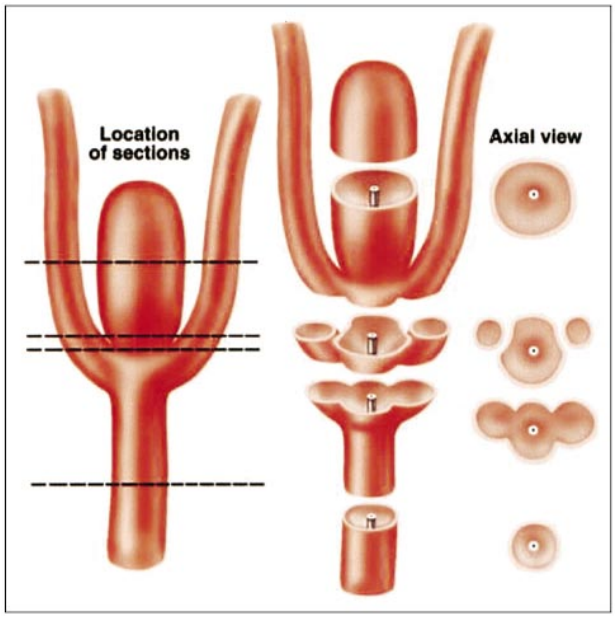

FIG 4. *Left,* Diagram of a bifurcation aneurysm, parent artery, and adjacent branches (*dashed lines* indicate locations at which intravascular sonographic measurements were made).

Center, Line drawings of sections through the parent artery, the aneurysm, and adjacent branches in the plane of intravascular sonography.

Right, Line drawing of corresponding intravascular sonograms.

determining the time that was required for the transducer to travel from the distal to the proximal extent of the ostium and then multiplying this time by the speed of the intravascular sonographic catheter pullback.

Measurements of each bifurcation aneurysm were made in the center of the dome, at the ostium, and in the parent artery by using electronic calipers (Fig 4). The third dimension of the ostia was calculated by determining from the video the time required to travel from the parent artery to a location at which there was clear demarcation of the walls of the aneurysm from the parent artery and then multiplying this time by the speed of the intravascular sonographic catheter pullback.

Two-dimensional Reformations

Initially, the intravascular sonograms were digitized from a half-inch super VHS videotape by means of an LG-3 frame grabber (Scion Corp, Frederick, MD) connected to a Power Macintosh computer with 160 MB of RAM at a rate of 30 frames (images) per second. The digitized data were collated into a volume stack using NIH Image 1.62 software (National Institutes of Health, Bethesda, MD). Digitization times varied from 20 to 45 seconds, depending on the catheter pullback time. Two-dimensional reformations of the volume data set were constructed easily by using the Reslice feature of the software program. The volume data set was reformatted through the center of the ostium to portray the maximal dimension in the plane being evaluated.

An accurate assessment of the distance between slices in pixel numbers was needed to ensure that the 2D reformatted images would have the correct aspect ratio. For a constant pullback rate of r mm/s, a total pullback time of t seconds, and a digitization frame rate of f frames per second, the distance, d_{mm}, in millimeters between slices is given by $d_{mm} = (r \cdot t)/(f \cdot t - 1)$. If the reformatted image is to have the correct aspect ratio, the number of pixels per millimeter in the pullback direction must equal the number of pixels per millimeter in the original image plane. Using the on-screen division markers in these images, the number of pixels between two markers was determined by using the NIH Image software. With the number of pixels per millimeter now known, it was a straightforward task to convert slice spacing in millimeters to pixels. Following this calculation, spatially accurate 2D reformations of the original data set were constructed. All images were saved in TIF format and archived on compact disks for later retrieval.

Results

In all instances, intravascular sonograms provided clear demarcation between the walls of the parent arteries, the aneurysm's ostia, and adjacent arterial branches. The intravascular sonographic catheters could easily be maneuvered either into or alongside all the aneurysms. Small vascular structures located in the tissue adjacent to the arteries being examined were well seen.

Lateral Aneurysms

In all lateral aneurysms, the width of the ostium could be measured, and in every case but one, the length of the ostium could be calculated. In the one exception, catheter instability caused by movement with systolic and diastolic flow made accurate determination of the ostium length impossible. The third dimension of the lateral aneurysms was negligible. In every instance, the intravascular sonograms provided a clear view of the demarcation between parent artery and aneurysm. This distinction between the limits of the parent artery and the aneurysm was less clearly defined on the angiographic images (Fig 5). Intravascular sonograms of the three lateral aneurysms that were examined after treatment with GDCs clearly depicted the location of the coils at the aneurysm's ostia as well as sites at which coils had not been positioned ad-

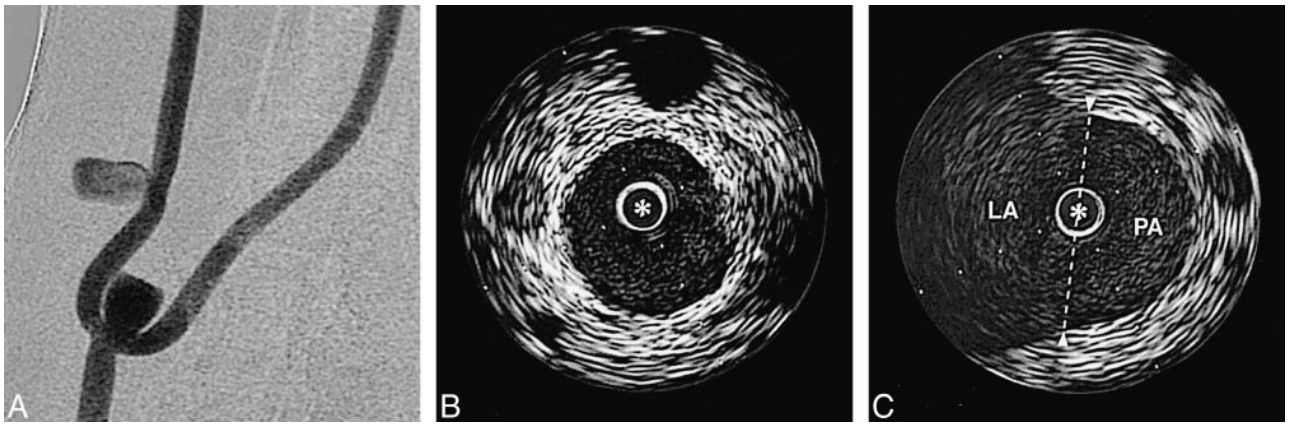

FIG 5. *A,* Angiogram of experimental aneurysm. The projection is optimized to allow best possible visualization of the lateral aneurysm's neck.

B, Intravascular sonogram of the parent artery that gives rise to the lateral aneurysm.

C, Intravascular sonogram through the lateral aneurysmal ostium. This image illustrates the ability to depict the width of the ostium (*arrowheads* indicate the point at which the lateral aneurysm, *LA,* joins the parent artery, *PA*; *dashed line* denotes the width of the ostium). In the intravascular sonograms, the distance between *white marker dots* is 1 mm and the intravascular sonographic catheter is defined by an *asterisk.*

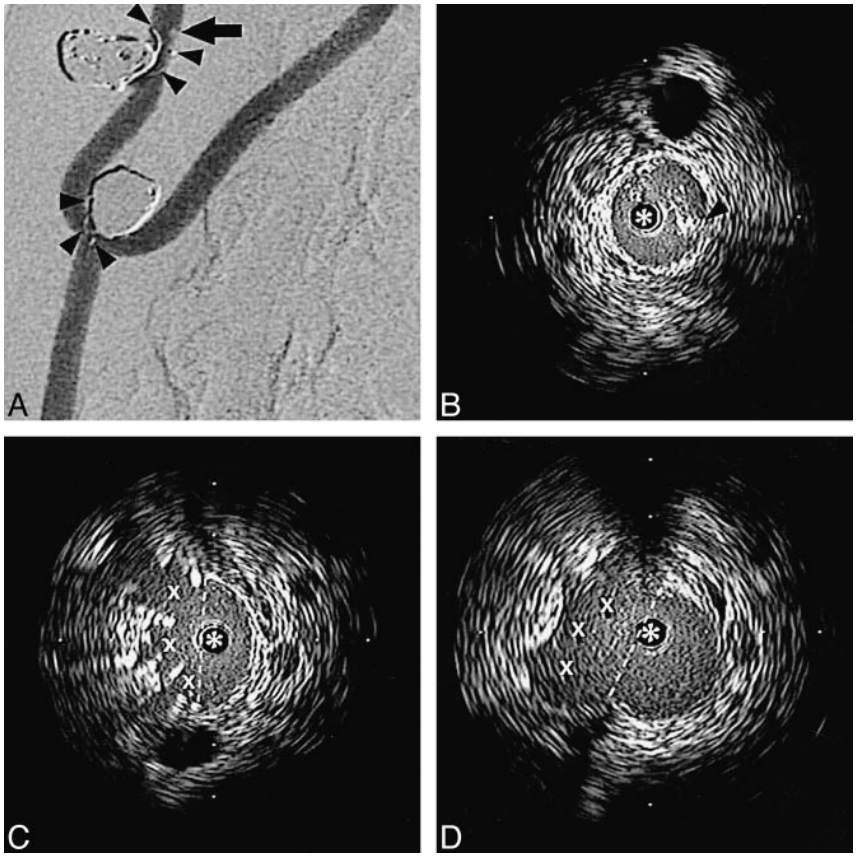

FIG 6. *A,* Angiogram of a lateral and a bifurcation aneurysm after treatment with GDCs. Coils are purposely positioned so as to protrude into the parent artery (*arrowheads*). A filling defect (*arrow*) along the wall of the parent artery of the lateral aneurysm represents thrombus.

B, Intravascular sonogram at the level of the filling defect on a DSA clearly shows the thrombus (*arrowhead*) as hyperechoic signal within the lumen.

C, Intravascular sonogram at the upper extent of the aneurysm's ostium shows coils filling the ostium (*dashed line* indicates limits of the aneurysmal ostium; *X*'s identify the spaces between coils).

D, Intravascular sonogram at the lower extent of the aneurysm's ostium shows a portion of the outflow tract that was not occluded (*X*) (*dashed line* defines the limits of the aneurysmal ostium). In the intravascular sonograms the distance between the *white marker dots* is 2 mm, and the intravascular sonographic catheter is defined by an *asterisk.*

equately to fill the aneurysm. Coils that had been purposely positioned so that they protruded into the parent artery were well seen on the intravascular sonograms. Intraluminal thrombus associated with some of these misplaced coils was also well defined. Although the DSA images showed both these findings, the degree of parent artery compromise and the full extent of the intraluminal thrombus were more clearly seen on the sonograms (Fig 6).

Bifurcation Aneurysms

With intravascular sonography, the dimensions of the bifurcation aneurysms, their ostia, and their relationship to the parent artery and adjacent branches were clearly seen in every instance. The length and width of the aneurysm's ostia could be directly measured; however, the third dimension of the ostia of the bifurcation aneurysms could only be estimated, since its extent was beyond (smaller

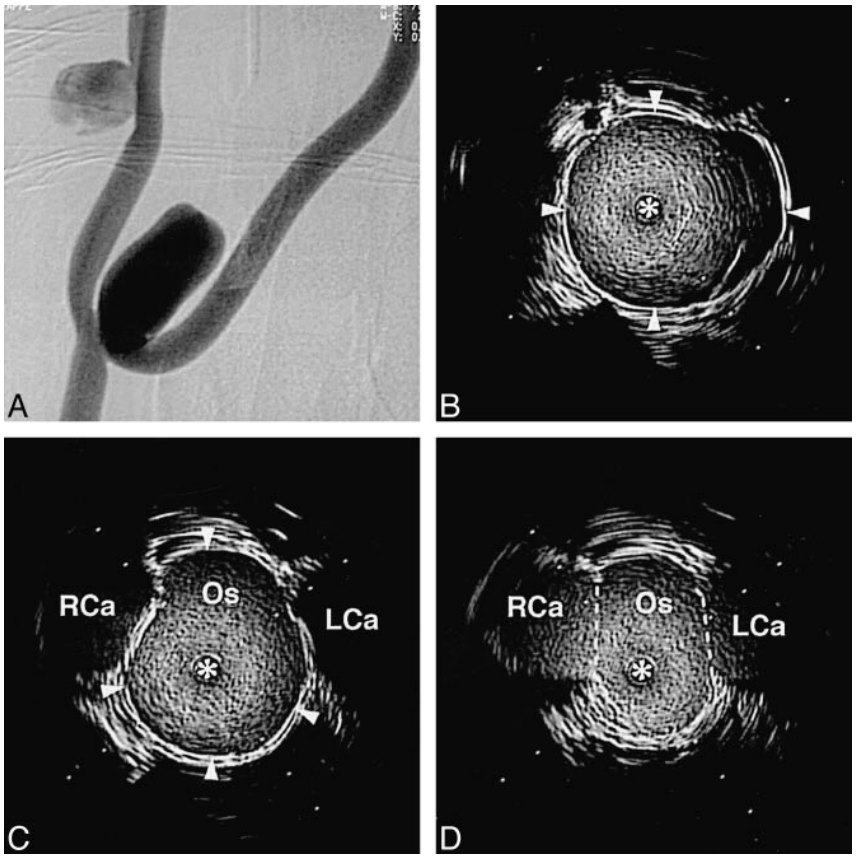

FIG 7. *A,* Angiogram of experimental aneurysms. The projection is optimized to allow visualization of the bifurcation aneurysm's neck.

B, Intravascular sonogram in the dome of the bifurcation aneurysm (*arrowheads* define the wall of the aneurysm).

C, Intravascular sonogram at a location just on the aneurysm side of the ostium (*Os*). The adjacent right and left carotid artery branches (*RCa* and *LCa,* respectively) are seen on either side of the aneurysm's wall as hypoechoic regions (*arrowheads* define the wall of the aneurysm).

D, Intravascular sonogram at the isthmus between the ostium (*Os*) and adjacent bifurcation branches (*dashed lines* indicate position at which ostium opens into the bifurcation of the left and right carotid arteries, *LCa* and *RCa,* respectively). In the intravascular sonograms the distance between *white marker dots* is 2 mm, and the intravascular sonographic catheter is defined by an *asterisk.*

than) the documented accuracy limits of the intravascular sonographic system. As is the case with the lateral aneurysm, this dimension is negligible. In one of these aneurysms, the ostia could not be seen on a single image but instead was seen during the acquisition of several frames. This was caused by an inability to shape the intravascular sonographic catheter so that the transducer was perpendicular to the plane of the ostium. Although the angiograms provided good definition of one dimension of these bifurcation aneurysm ostia, the intravascular sonograms were superior in allowing precise determination of both the shape (ie, length and width) of the ostia and their relationship to adjacent vessels (Fig 7). The rotational angiograms obtained in two of these experiments were only helpful in determining optimal projections for visualization of the relationship between an aneurysm and its parent artery.

Two-dimensional Reformats

The 2D reformatted images helped to clarify the spatial relationship between the aneurysm, its parent vessel, and adjacent branches. These reformatted images allowed direct determination of the dimensions of the aneurysm's ostia that previously had to be calculated. Although artifacts caused by pulsatile blood flow and cardiac motion degraded the reformatted images, they were still of diagnostic quality (Figs 8 and 9).

Statistics

When comparing the measurements made on two separate occasions by each author of the size of the parent vessel lumen and the aneurysm's ostium, strong inter- and intraobserver correlation was found (Fig 10).

Discussion

The major determinant required for successful endovascular treatment of saccular aneurysms with GDCs is the ability to accurately depict the aneurysm's neck and its relationship to the parent artery and adjacent branches. Aneurysms that have a small neck (ie, one that does not incorporate adjacent branches) can now be treated safely and effectively with GDCs (1, 7). Correlation between neck size (an extraluminal morphologic feature) and ostium dimensions (an intraluminal morphologic feature) has, to our knowledge, only been established by inference, with large aneurysm's necks assumed to be associated with large ostia and small necks associated with small ostia. In fact, characterizations of aneurysm's necks as small or large are based on traditional concepts derived both from direct surgical observations and classical angiographic analyses. Neither method allows consistent determination of a second or third dimension of the neck. Relationships between neck size and ostium configuration (eg, circular vs elliptical) are not defined. Like neck size, this morphologic feature

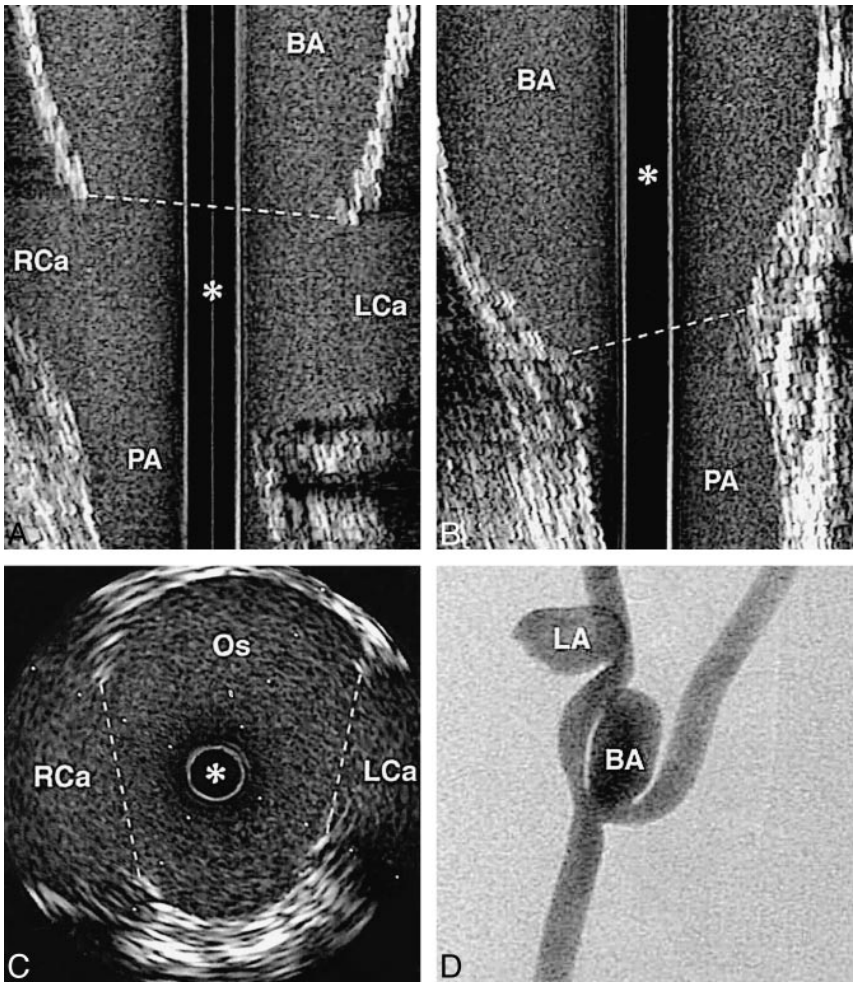

FIG 8. *A–D,* 2D reformations of a bifurcation aneurysm in the coronal (*A*) and sagittal (*B*) planes with corresponding axial image at the ostium (*C*) and a DSA (*D*) (*dashed lines* indicate the limit of the ostium; *BA,* bifurcation aneurysm; *PA,* parent artery; *RCa,* right carotid artery; *LCa,* left carotid artery; *Os,* ostium; *asterisk* denotes the intravascular sonographic catheter).

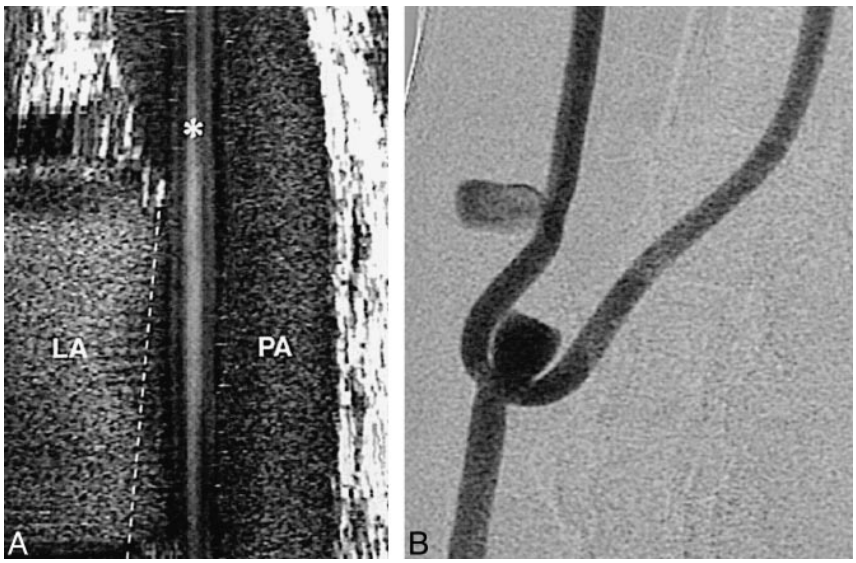

FIG 9. *A,* 2D reformation of a lateral aneurysm in the coronal plane. The artifact in this image is caused by up-and-down motion of the intravascular sonographic catheter during the cardiac cycle (*asterisk* denotes the intravascular sonographic catheter; *LA,* lateral aneurysm; *PA,* parent artery; *dashed line* identifies the limit of the aneurysm ostia).

B, Corresponding DSA.

might impact significantly on the ability to effectively use GDCs (eg, an aneurysm with an 8 × 2-mm ostium would be more suitable for treatment with GDCs than would an aneurysm with an 8 × 8-mm ostium). Because of inherent differences between the technique of aneurysm clipping (an extraluminal approach) and endovascular treatment (an endoluminal approach), the ability to characterize these features of an ostium theoretically assumes greater importance when planning endovascular treatment than when contemplating surgical clipping.

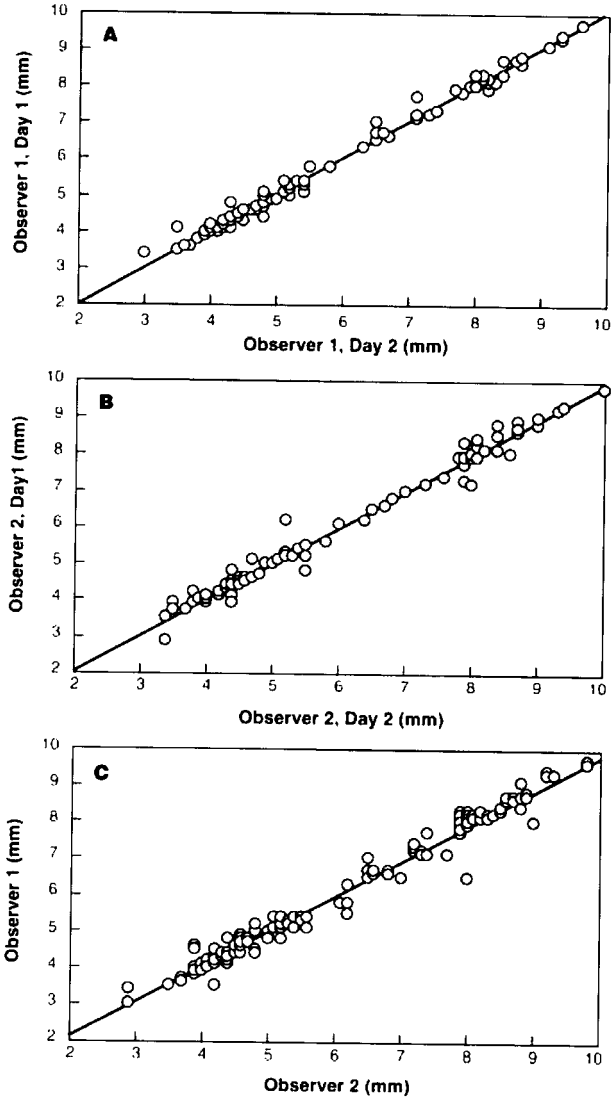

FIG 10. Regression plots of inter- and intraobserver correlation coefficients ($P < .0001$ in each instance).

When aneurysms are large, have a complex shape, or are located at a bifurcation at which vascular branching is complex, it is often difficult or even impossible to define these morphologic features by using currently available angiographic methods (1). Although DSA remains the reference standard for the diagnostic evaluation of cerebral aneurysms, other techniques, such as MR angiography and CT angiography, are increasingly being used. These techniques are of limited use when aneurysms are small (<4–5 mm), when flow is slow or disturbed, when an aneurysm is adjacent to bone or a dural sinus, or when there is patient motion (8, 9). A recent article has reported that, as compared with DSA, 3D CT angiography is able to define aneurysm neck size with accuracy to within 2 mm (10); however, only one dimension of the neck was measured and rigorous validation of the accuracy of this technique has not been reported. The limitations of DSA in defining complex vascular relationships have been well described (ie, a 2D solution to a 3D problem) (11). While 3D acquisitions using traditional DSA techniques are now becoming available (12), to our knowledge, in no case has the ability of any of these techniques to define accurately the intraluminal morphologic features of aneurysm ostia or their relationship to adjacent branches been described. In addition, we know of no published studies comparing these endovascular reconstructions with anatomic specimens or models in order to define the accuracy of measurements of anatomic structures on CT or MR angiograms or on DSA 3D reconstructions.

Numerous studies have validated the ability of intravascular sonography to depict accurately vessel morphology in normal as well as in tortuous and diseased vessels (13–17). The accuracy of using a motorized pullback servo device in combination with intravascular sonography to determine length has also been validated (18). The manufacturer guarantees the accuracy of measurements made with each catheter used in this study to be within 10%. This ability to determine vascular dimensions and morphology easily and accurately has stimulated increasing reports of the use of intravascular sonography in conjunction with therapeutic endovascular procedures both in the coronary and the peripheral vasculature (14, 15, 19–21). Of particular importance are reports describing the value of combining intravascular sonography with therapeutic interventions in the coronary circulation (20, 21).

In this study we have demonstrated that intravascular sonograms can depict all dimensions of an aneurysm's ostium as well as its relationship to adjacent branches. Similar information was not obtained from DSA images, even when rotational DSA was used. Our intra- and interobserver correlations exceeded the manufacturer's specified accuracy for the intravascular sonographic device (ie, $\pm$10%). This ability to observe the relationships between an aneurysm, its parent artery, and adjacent branches from an endoluminal rather than an extraluminal perspective is, from the viewpoint of the endovascular therapist, a fundamental advantage of intravascular sonography over traditional DSA.

Owing to mechanical limitations of transducer construction, intravascular sonograms are oriented in a plane perpendicular (ie, axial) to the long axis of the imaging catheter or wire. This orientation makes it easy to measure the diameter of an aneurysm's parent artery (Fig 5). When the transducer is introduced through an aneurysm's ostium, the length and width can be measured directly (Fig 7). In circumstances in which the transducer cannot be introduced through an aneurysm's ostium, the width of the ostium can be measured directly and the length can be calculated by multiplying the time required for the transducer to be pulled across the ostium by the speed of the pullback (Fig 5). The third dimension of an aneurysm's ostium (ie,

height) is negligible both in experimental and human aneurysms.

Because only information from the axial plane is displayed at one time, the longitudinal perspective of the vessel morphology must be mentally integrated by the operator. To overcome this obstacle, attempts at providing on-line 2D and 3D reconstructions are being undertaken (22–24). We found 2D reformations to be especially helpful in evaluating features of the aneurysm that are not seen directly; that is, the length of the lateral aneurysm and the height (the third dimension) of both lateral and bifurcation aneurysms (Fig 8 and 9). The multiplanar capability of 2D reformats helps clarify the spatial relationships of the aneurysm's ostium and adjacent arterial branches. Postprocessing of intravascular sonographic data for 2D reformations or 3D reconstructions is possible, and when easily available will simplify the demonstration of ostia dimensions as well as the relationships of adjacent vessels.

Our study also shows the ability of intravascular sonography to depict the position of coils placed across an aneurysm's ostium. This allows recognition not only of incomplete aneurysm occlusion or compromise of the parent artery by coils but also clear visualization of thrombus within a parent artery. Although the role of intravascular sonography in clinical practice remains to be determined, it is our opinion that its ability to define aneurysm morphology more fully will most likely contribute significantly to identification of those aneurysms that are appropriate for treatment with GDCs.

Conclusion

Intravascular sonography is a novel technique for visualizing the ostium (neck) of an aneurysm. It provides complete morphologic delineation of the size of the aneurysm's ostium and the relationship of the ostium to adjacent arterial branches—information that is not obtainable with the use of any other currently available imaging technique. In conjunction with DSA, intravascular sonography opens another window through which to monitor and control endovascular therapeutic procedures.

Acknowledgment

We acknowledge the valuable contribution of Allan Rappe to this study.

References

1. Cognard C, Weill A, Castaings L, Rey A, Moret J. **Intracranial berry aneurysms: angiographic and clinical results after endovascular treatment.** *Radiology* 1998;206:499–510
2. Malisch T, Guglielmi G, Vinuela F, et al. **Intracranial aneurysms treated with the Guglielmi detachable coil: midterm results in a consecutive series of 100 patients.** *J Neurosurg* 1997;87:176–183
3. Graves VB, Strother CM, Duff TA, Perl J. **Early treatment of ruptured aneurysms with Guglielmi detachable coils: effect on subsequent bleeding.** *Neurosurgery* 1995;37:640–648
4. Fernandez Zubillaga A, Guglielmi G, Vinuela F, Duckwiler GR. **Endovascular occlusion of intracranial aneurysms with electrically detachable coils: correlation of aneurysm neck size and treatment results.** *AJNR Am J Neuroradiol* 1994;15:815–820
5. German WJ, Black PW. **Experimental production of carotid aneurysms.** *N Engl J Med* 1954;250:104–106
6. Strother CM, Graves VB, Rappe A. **Aneurysm hemodynamics: an experimental study.** *AJNR Am J Neuroradiol* 1992;13:1089–1095
7. Vinuela F, Duckwieler G, Mawad M. **Guglielmi detachable coil embolization of acute intracranial aneurysm: perioperative anatomical and clinical outcome in 403 patients.** *J Neurosurg* 1997;86:475–482
8. Harrison MJ, Johnson BA, Gardner GM, Welling BG. **Preliminary results on the management of unruptured intracranial aneurysms with magnetic resonance angiography and computed tomographic angiography.** *Neurosurgery* 1997;40:947–957
9. Ogawa T, Okudera T, Noguchi K, et al. **Cerebral aneurysms: evaluation with three-dimensional CT angiography.** *AJNR Am J Neuroradiol* 1996;17:447–454
10. Hope JKA, Wilson JL, Thomson FJ. **Three-dimensional CT angiography in the detection and characterization of intracranial berry aneurysms.** *AJNR Am J Neuroradiol* 1996;17:439–445
11. Minesh PM, Petereit D, Turski P, Gehring M, Levin A, Kinsella T. **Magnetic resonance angiography: a three dimensional database for assessing arteriovenous malformations (technical note).** *J Neurosurg* 1993;79:289–293
12. Schueler BA, Sen A, Hsiung H, Latchaw RE, Hu X. **Three-dimensional vascular reconstruction with a clinical X-ray angiography system.** *Acad Radiol* 1997;4:693–699
13. Lockwood GR, Ryan LK, Gotlieb AI, et al. **In vitro high resolution intravascular imaging in muscular and elastic arteries.** *J Am Coll Cardiol* 1992;20:153–160
14. Nishimura RA, Edwards WD, Warnes CA, et al. **Intravascular ultrasound imaging in vitro validation and pathologic correlation.** *J Am Coll Cardiol* 1990;16:145–154
15. Manninen HI, Rasanen H, Vanninen RL, et al. **Human carotid arteries: correlation of intravascular US with angiographic and histopathologic findings.** *Radiology* 1998;206:65–74
16. Pandian NG, Kreis A, Brockway B, et al. **Ultrasound angioscopy: real-time two-dimensional, intraluminal ultrasound imaging of blood vessels.** *Am J Cardiol* 1988;62:493–494
17. Junbo G, Fengqi L, Peter K, et al. **Intravascular ultrasound approach to the diagnosis of coronary artery aneurysms.** *Am Heart J* 1995;130:765–771
18. Fuessl RT, Mintz GS, Pichard AD, et al. **In vivo validation of intravascular ultrasound length measurements using a motorized transducer pullback device.** *Am J Cardiol* 1996;77:1115–1118
19. Waller BF, Pinkerton CA, Slack JD. **Intravascular ultrasound: a histological study of vessels during life—the new "gold standard" for vascular imaging.** *Circulation* 1992;85:2305–2310
20. Abizaid A, Mintz GS, Pichard AD, et al. **Is intravascular ultrasound clinically useful or just a research tool?** *Heart* 1997;78(Suppl 2):27–30
21. Nakamura S, Colombo A, Gaglione A, et al. **Intracoronary ultrasound observations during stent implantation.** *Circulation* 1994;89:2026–2034
22. von Birgelen C, deVrey E, Mintz G, et al. **ECG-gated three-dimensional intravascular ultrasound: feasibility and reproducibility of the automated analysis of coronary lumen and atherosclerotic plaque dimensions in humans.** *Circulation* 1997;96:2944–2952
23. von Birgelen C, Mintz G, Nicosia A, et al. **Electrocardiogram-gated intravascular ultrasound image acquisition after coronary stent deployment facilitates on-line three-dimensional reconstruction and automated lumen quantification.** *J Am Coll Cardiol* 1997;30:436–443
24. Evans JL, Ng KH, Wiet SG, et al. **Accurate three-dimensional reconstruction of intravascular ultrasound data: spatially correct three-dimensional reconstructions.** *Circulation* 1996;93:567–576